Journal of proteome research

pubs.acs.org/jpr

Article

Maternal Rat Metabolomics: Amniotic Fluid and Placental Metabolic Profiling Workflows

Alexandra Bourdin-Pintueles, Laurent Galineau, Lydie Nadal-Desbarats, Camille Dupuy, Sylvie Bodard, Julie Busson, Antoine Lefèvre, Patrick Emond, and Sylvie Mavel*

Cite This: https://doi.org/10.1021/acs.jproteome.1c00145

Read Online

ACCESS | Metrics & More | Article Recommendations | Supporting Information

ABSTRACT: Studying the metabolome of specific gestational compartments is of growing interest in the context of fetus developmental disorders. However, the metabolomes of the placenta and amniotic fluid (AF) are poorly characterized. Therefore, we present the validation of a fingerprinting methodology. Using pregnant rats, we performed exhaustive and robust extractions of metabolites in the AF and lipids and more polar metabolites in the placenta. For the AF, we compared the extraction capabilities of methanol (MeOH), acetonitrile (ACN), and a mixture of both. For the placenta, we compared (i) the extraction capabilities of dichloromethane, methyl *t*-butyl ether (MTBE), and butanol, along with (ii) the impact of lyophilization of the placental tissue. Analyses were performed on a C18 and hydrophilic interaction liquid chromatography combined with high-resolution mass spectrometry. The efficiency and the robustness of the extractions were compared based on the number of the features or metabolites (for untargeted or targeted approach, respectively), their mean total intensity, and their coefficient of variation (% CV). The extraction capabilities of MeOH and ACN on the AF metabolome were equivalent. Lyophilization also had no significant impact and usefulness on the placental tissue metabolome profiling. Considering the placental lipidome, MTBE extraction was more informative because it allowed extraction of a slightly higher number of lipids, in higher concentration. This proof-of-concept study assessing the metabolomics and lipidomics of the AF and the placenta revealed changes in both metabolisms, at two different stages of rat gestation, and allowed a detailed prenatal metabolic fingerprinting.

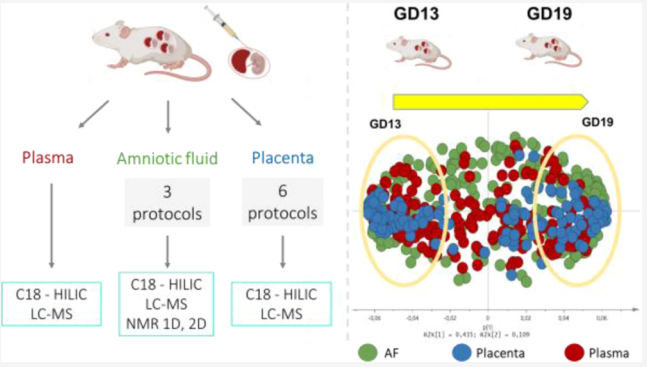

KEYWORDS: *LC-MS, NMR, targeted, untargeted, lipidomics, fingerprinting methodology, validation, pregnant rodent*

1. INTRODUCTION

Metabolomics allows for the detection, identification, and quantification of small molecules (below 1 kDa) such as amino acids, hormones, and sugars in human, animal, vegetal, and cell samples. The amount of these compounds, called the metabolome, reflects the metabolism of the organism as they represent substrates, intermediates, and products of multiple biochemical pathways. Thus, metabolomics is increasingly used for biomarker discovery and establishing pathophysiological metabolome signatures and used in diagnosis, pharmacological treatment research, and toxicological studies.[1] Metabolomics studies have been optimized on several matrices such as urine, serum/plasma, or feces samples.[2] However, specific pathophysiological contexts require investigating other matrices. To date, there is a growing interest for using metabolomics in the context of neurodevelopmental disorders to find biomarkers for an early diagnosis.[3,4] In this context, metabolomics of other matrices at the interface between the mother and the developing child such as amniotic fluid (AF)[5] and placenta[4,6] is of a great interest but still poorly documented.[7] In fact, the metabolism of AF reflects the physiological processes of fetal development[8,9] and as an interface between the mother and the fetus, the placenta performs multiple functions to support pregnancy functions and a normal fetal development.[10] Altogether, this makes the metabolomics of the placenta and AF an extremely valuable material for fetal health diagnostics.

Several studies have explored the metabolome of the AF[5,11−14] and the placenta.[15−17] However, there is still a lack of information related to their characterization and on the best suited methodology to study these matrices. Our objective was to develop an exhaustive and robust method to study the AF and placental metabolomes along with the placental lipidome using pregnant rat samples to obtain a global profiling of these

Received: February 19, 2021

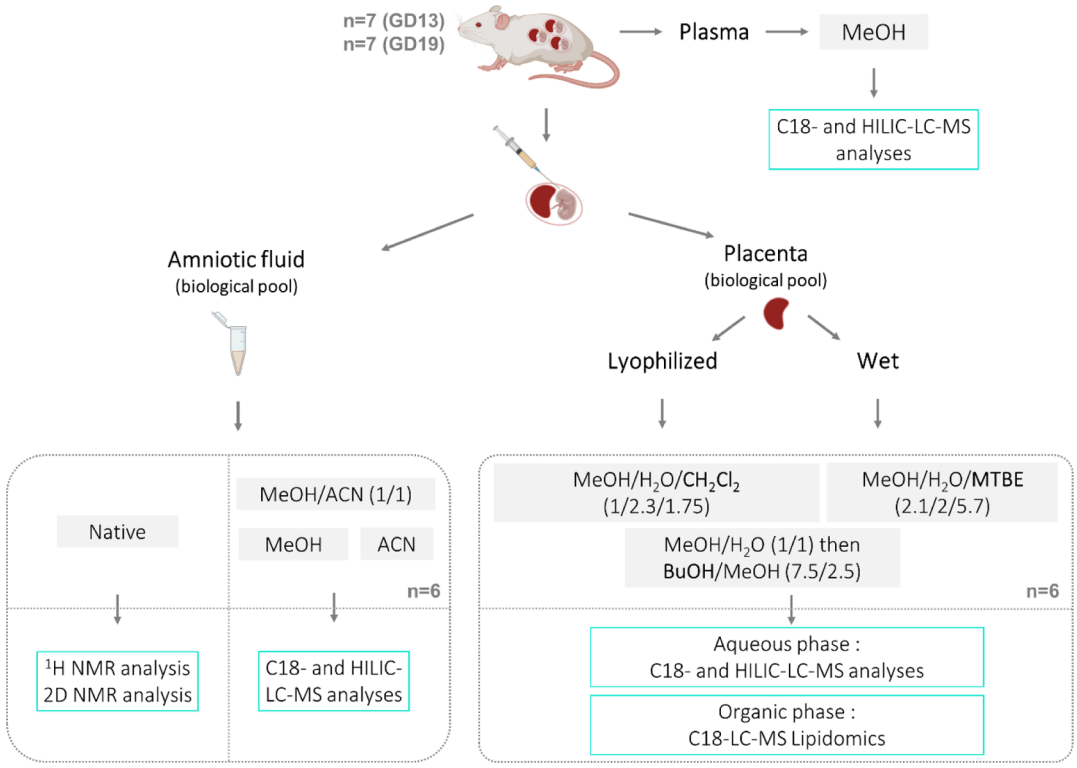

Figure 1. Workflow protocol for optimization of AF and placenta preparation, extraction, and analytical processes.

two compartments. We investigated the AF metabolome using three solvent extraction protocols analyzed by (i) ultrahigh-performance liquid chromatography with high-resolution mass spectrometry (UHPLC−HRMS) with two chromatographic columns, C18 and hydrophilic interaction liquid chromatography (HILIC), and (ii) nuclear magnetic resonance (NMR). Regarding the placenta, the impact of working on frozen or lyophilized samples was investigated and three solvent extractions were compared. The lipidomics (study of lipid metabolism) was performed using reverse-phase liquid chromatography with mass spectrometry (RP−LC−MS), and from this extraction, the more polar metabolome was investigated by C18- and HILIC−LC−MS. In addition to the multiplatform analyses, a targeted and a nontargeted approach were both used in order to expose a global view of the metabolome of these matrices.

Finally, a proof-of-concept study was performed using the defined optimal conditions to study the evolution and complementarity of the AF and placental metabolomes at two gestational stages. Gestational stages 13 and 19 correspond to late embryonic and fetal stages in rats, respectively.[18] These two gestational time points were chosen to observe modifications in the metabolisms of maternal and fetal matrices during these two key periods of gestation as potential tools for biological studies.

2. EXPERIMENTAL SECTION

2.1. Animals

All animal experiments were conducted in accordance with local and international guidelines and approved by a local ethics committee. A total of 14 pregnant female Wistar rats were purchased (Janvier Labs, Le Genest St. Isle, France) and were individually housed under humidity- and temperature-controlled conditions and a 12:12 light−dark cycle (light on at 7.00 AM) with access to food and water *ad libitum*. Rats were randomly distributed into 2 groups of 7 females: GD13 group and GD19 group, corresponding to the day of sacrifice by decapitation at 13 and 19 gestational days, respectively. Each female had between 10 and 12 fetuses (Figure 1).

2.2. Sample Collection and Storage

Blood (1 mL) was collected from each female after decapitation in a 1.5 mL Eppendorf tube containing 1.8 mg/mL of ethylenediaminetetraacetic acid, centrifuged at 5000*g* for 20 min at 4 °C, and stored at −80 °C. After the cesarean section, the AF of each gestational sac was collected with a 1 mL syringe and a 26-gauge needle, pooled into two 1.5 mL Eppendorf tubes (to give a biological pool used for all the experiments), and stored at −80 °C. The placenta of each gestational sac was also collected, rinsed with saline, pooled into two 1.5 mL Eppendorf tubes, and stored at −80 °C.

2.3. UHPLC−HRMS Analyses

2.3.1. Amniotic Fluid. Metabolites were extracted with three different methods. The AF (150 μL of the biological pool) was mixed with 20 μL of internal standards (IS) (a mixture of 7 drugs: fenofibrate, sulfapyridine, secobarbital, phenobarbital, cethexonium bromide, promethazine, and sulfanilamide) and 400 μL of either methanol (MeOH), acetonitrile (ACN), or methanol/ACN (1:1) (n = 6 replicates each). Samples were vortexed for 5 s and incubated at −20 °C for 30 min. Then, samples were centrifuged at 5000*g* at 4 °C for 15 min, and 410 μL of the supernatant was retrieved. A second extraction was performed, and the cumulative 820 μL collected was equally subdivided into half for future C18 and HILIC analyses, evaporated at 40 °C using a SpeedVac concentrator, and stored at −80 °C until LC−MS analysis. Then, the best protocol was tested on seven individually collected samples at GD13 and GD19.

https://doi.org/10.1021/acs.jproteome.1c00145
J. Proteome Res. XXXX, XXX, XXX−XXX

2.3.2. Placenta. For placental tissue, we compared three extraction methods on either wet or lyophilized tissue. Frozen placenta pool was homogenized with an Ultra Turrax (Ika, Staufen, Germany) at 20,000 rpm for 5 min. Then, 18 × 40 mg was weighed in Eppendorf tubes and stored at −80 °C until extraction. The remainder was lyophilized during 48 h in a FreeZone lyophilizer (Labconco, Kansas City, MO, USA). From the resulted fine powder, 18 × 6 mg (corresponding to approximately 40 mg of wet tissue) was weighed in Eppendorf tubes followed by the extraction process.

The modified Bligh-Dyer, Matyash, and Butanol/Methanol (BUME) methods were tested to extract both metabolome and lipidome.

(A) 1 mL of MeOH/H_2O (milli-Q) (1:1) (n = 6 replicates each) was added to 40 mg of wet tissue or to 6 mg of lyophilized tissue. Samples were vortexed for 2 min, incubated for 20 min at −20 °C, and supplemented with 340 μL of dichloromethane (CH_2Cl_2) and 30 μL of a solution of IS. CH_2Cl_2 was used instead of chloroform due to its lower toxicity and its similar properties.[19] After homogenization, samples were centrifuged at 5,000g at 4 °C for 15 min. The upper phase (660 μL) was removed and kept in vials. Then, a second extraction with 990 μL of CH_2Cl_2/ACN/H_2O (milli-Q) (1:1:1) was performed. The upper phase (400 μL) was removed, added to the precedent 660 μL, and then equally separated for future C18 and HILIC analyses, while the lower phase was put into vials for lipidomics analysis.

(B) 330 μL of MeOH (n = 6 replicates each) was added to 40 mg of wet tissue or 6 mg of lyophilized tissue. Samples were vortexed for 2 min, incubated at −20 °C for 20 min, and supplemented with 1.2 mL of methyl *tert*-butyl ether (MTBE)/H_2O (milliQ) (2:1) and 30 μL of IS. After homogenization, samples were centrifuged at 5000g at 4 °C for 15 min. The upper phase (600 μL) was removed and kept for lipidomics analysis. A second extraction with 900 μL of MTBE/MeOH/H_2O (milli-Q) (6:2:1) was performed. The upper phase (400 μL) was removed and added to the previous 600 μL, while the lower phase was equally separated for C18 and HILIC analyses.

(C) 500 μL of MeOH/H_2O (milli-Q) (1:1) and 30 μL of IS (n = 6 replicates each) were added to 40 mg of wet tissue or 6 mg of lyophilized tissue. Samples were vortexed for 2 min, incubated at −20 °C for 20 min, and centrifuged at 5000g at 4 °C for 15 min. The supernatant (400 μL) was collected into vials. A second extraction with 1 mL of MeOH/H_2O (milli-Q) (1:1) was performed. The supernatants (800 μL) were added to the precedent 400 μL and then subdivided for future C18 and HILIC analyses. Then, 500 μL of BuOH/MeOH (milli-Q) (0.75:0.25) was added to the pellet to extract lipids. After homogenization, samples were centrifuged at 5000g at 4 °C for 15 min, and the supernatant (300 μL) was collected into vials. A second extraction was performed and 300 μL of supernatant was added to the first ones for lipidomics analysis. Samples were evaporated at 40 °C using a SpeedVac concentrator and stored at −80 °C until LC−MS analysis.

2.3.3. Plasma. Plasma (50 μL) was mixed with 20 μL of IS and 400 μL of cold MeOH, vortexed for 5 s, and incubated for 30 min at 4 °C. Samples were centrifuged at 5000g for 25 min at 4 °C. The supernatant (350 μL) was equally subdivided into half for future C18 and HILIC analyses, and samples were evaporated at 40 °C using a SpeedVac Concentrator and stored at −80 °C until LC−MS analysis.

2.3.4. UHPLC−HRMS Parameters. The aqueous fractions of AF, placenta, and plasma were reconstituted with 100 μL of H_2O (milli-Q)/MeOH (9:1) for C18 and 100 μL of ACN/H_2O (milli-Q) (9:1) for HILIC. The liposoluble fractions of the placenta were reconstituted with 100 μL of a 6:3:1 mix of ACN/H_2O/isopropanol before LC−MS. LC−MS analysis was performed as previously described.[20,21] Briefly, a UHPLC Ultimate 3000 system (Dionex, Sunnyvale, CA, USA), coupled to a Q-Exactive quadrupole-orbitrap-MS (Thermo Fisher Scientific, San Jose, CA, USA), was operated in the positive electrospray ionization (ESI+) and negative electrospray ionization (ESI−) mode. For C18−LC−MS analysis, chromatography was carried out with a 1.7 μm C18−XB (150 mm × 2.10 mm, 100 Å) UHPLC column (Kinetex, Phenomenex, Torrance, CA, USA) heated at 55 °C. The solvent system comprised mobile phase A (H_2O + 0.1% formic acid) and mobile phase B (MeOH + 0.1% formic acid); the gradient was operated at a flow rate of 0.4 mL/min over a run time of 26 min. The multistep gradient was programmed as follows: 0 to 6 min, 99.9% A; 6 to 10 min, 75% A; 10 to 12 min, 20% A; 12 to 14 min, 10% A; 14 to 17 min, 0.1% A; 17 to 20 min, 99.9% A; and 21 to 24 min, 99.9% A. For HILIC−LC−MS analysis, chromatography was carried out with a 1.7 μm Cortecs HILIC-virgin silica (150 mm × 2.10 mm, 100 Å) UHPLC column (Waters) heated at 40 °C. The solvent system comprised mobile phase A (H_2O + 0.5% formic acid + 10 mM ammonium formate) and mobile phase B (ACN + 0.5% formic acid + 10 mM ammonium formate); the gradient was operated at a flow rate of 0.4 mL/min over a run time of 23 min. The multistep gradient was programmed as follows: 0 to 8 min, 5% A; 8 to 15 min, 18% A; 15 to 15.5 min, 25% A; 15.5 to 16 min, 75% A; 16 to 18.1 min, 97% A; and 18.1 to 23 min, 5% A. For lipidomics analysis, chromatography was carried out with a 1.7 μm Kinetex C18 (150 mm × 2.10 mm, 100 Å) UHPLC column (Phenomenex) heated at 55 °C. The solvent system comprised mobile phase C [isopropanol/ACN (9:1) + 0.1% (v/v) formic acid + 10 mM ammonium formate] and mobile phase D [ACN/H_2O (6:4) + 0.1% (v/v) formic acid + 10 mM ammonium formate]; the gradient was operated at a flow rate of 0.260 mL/min over a run time of 30 min. The multistep gradient was programmed as follows: 0 to 1.5 min, 32% C; 1.5 to 5 min, 45% C; 5 to 8 min, 52% C; 8 to 11 min, 58% C; 11 to 14 min, 66% C; 14 to 18 min, 70% C; 18 to 21 min, 75% C; 21 to 24 min, 97% C; and 24 to 30 min, 32% C. The autosampler temperature (Ultimate WPS-3000 UHPLC system, Dionex) was set at 4 °C, and the injection volume for each sample was 5 μL. During the full-scan acquisition, which ranged from 250 to 1600 m/z, the instrument was operated at 70,000 resolution.

The instrumental stability was evaluated by multiple injections (n = 5) of a quality control (QC) sample obtained from a pool of 10 μL of all samples of one matrix. This QC sample was injected at the beginning of the analysis, between every 10 sample injections, and at the end of the run.[22,23] Two diluted QC sample dilutions (to 1/2 and to 1/4) were studied to determine the linearity of the dilution curves, showing the robustness of a metabolite analysis. A blank was injected at the beginning and at the end of the run.[24]

https://doi.org/10.1021/acs.jproteome.1c00145
J. Proteome Res. XXXX, XXX, XXX−XXX

Table 1. Reproducibility Assesment of Metabolites Detected in AF in C18 and HILIC LC−MS Targeted Analyses in ESI ± Modes (n = 6 Replicates)

AF−targeted analysis	MeOH		ACN		MeOH/ACN	
	C18 ESI+/−	HILIC ESI+/−	C18 ESI+/−	HILIC ESI+/−	C18 ESI+/−	HILIC ESI+/−
mean total intensity (standard deviation)	1.45×10^{10} (4.5×10^{8})	6.16×10^{9} (2.3×10^{8})	1.34×10^{10} (3.7×10^{8})	3.83×10^{9} (1.6×10^{8})	1.33×10^{10} (9.9×10^{8})	7.34×10^{9} (1.5×10^{9})
total metabolites	197	170	193	162	195	165
number of reproducible metabolites (CV < 30%)	167	139	167	122	157	108
percentage of reproducible metabolites	85%	82%	87%	75%	81%	65%
mean of % CV from reproducible metabolites	8.5	11.6	8.5	13.7	7.7	16.5

2.4. NMR

NMR 1D was performed as previously described.[25] Briefly, a pool of AF was thawed, and 150 μL (or 100 or 50 μL for robustness study through analysis of the linearity of dilution curves) was added q.s. (quantum satis) 200 μL of 0.2 M potassium phosphate buffer in deuterium oxide (D_2O) 99%. A total of 8 μL of 3-trimethylsilylpropionic acid (0.05 wt % in D_2O) was added to samples as an internal reference. After centrifugation, the supernatant was transferred to 3 mm NMR tubes. The NMR spectra were obtained with a BrukerDRX-600 AVANCE-III HD spectrometer (Bruker SADIS, Wissembourg, France), operating at 14 T, with a TCI cryoprobe (Bruker SADIS). ^{1}H NMR spectra were acquired using a "noesypr1d" pulse sequence with a relaxation delay of 10 s. ^{1}H spectra were collected with 128 scans. A "Hsqcetgp" pulse sequence for 2D (^{1}H−^{13}C) NMR was used with 4096 × 256 data points using 64 scans per increase, with a relaxation time of 2.5 s. Resolution-enhanced spectra were obtained, without loss of sensitivity, using a nonuniform sampling (NUS) approach. NUS spectra are faster to acquire than conventional ones,[26] in our case 3 h.

2.5. Data Processing

2.5.1. LC−MS. For the LC−MS targeted approach, a library of 495 standard compounds (Mass Spectroscopy Metabolite Library of Standards MSMLS, IROA Technologies) was analyzed with the same gradient of mobile phases and under the same conditions than those used for this study. In order to validate the identity of detected metabolites, the retention time must be within 6−20 s of the standard reference, the measured molecular mass of the metabolite must be within 10 ppm of the known mass of the reference compound and the isotope ratios of the metabolite must match the standard reference. The signal was calculated using Xcalibur software (Thermo Fisher Scientific) by integrating selected ion chromatographic peak area.

For the untargeted approach, data were analyzed using Workflow4Metabolomics (W4M), an online platform including XCMS.[27] A preprocessing workflow was created in our laboratory following the global steps: (1) CentWave-chromatographic peak detection with a max tolerated ppm m/z deviation of 15.0 and a minimum difference in m/z of 0.008 for the extraction method, (2) alignment method by grouping chromatographic peaks within and between samples by PeakDensity with a bandwidth of 10 and using Obuwrap for the retention time correction. Only the $[M + H]^+$ ion was kept for further analysis.

Only metabolites/features detected in 80% of repetitions were kept for further analysis. Data were normalized to the total area of peaks of interest, metabolites, and lipids with CV > 30% in QC and not respecting the dilution law were ejected.[24] The list of the annotated metabolites is given in Supporting Information (Table S1).

2.5.2. NMR. Data were analyzed as previously described.[28] NMR spectra were processed using TopSpin version 3.6.1 software (Bruker Daltonik, Karlsruhe, Germany). Identification of metabolites was achieved using Chenomx software (Chenomx Inc, Edmonton, Canada). 2D spectra were processed using MestReNova version 7.1.0 software (Mestrelab Research, Santiago de Compostela, Spain) as previously described.[29] The signals were assigned using the Metabominer software[30] with tolerances of 0.05 ppm (^{1}H) and 0.1 ppm (^{13}C).

2.5.3. Statistical Analysis. The coefficient of variation (% CV) was calculated as the ratio of the standard deviation to the mean and multiplied by 100. Nonparametric tests (Wilcoxon rank-sum test) were obtained from the Metaboanalyst web site (www.metaboanalyst.ca), the false discovery rate (FDR)-corrected p values were provided.[31] Unsupervised multivariate analysis [principal components analysis (PCA)] was performed as previously described using Simca-P + -15 software (Umetrics, Umeå, Sweden).[32] Venn diagrams were performed using the free software Hello jvenn![33]

3. RESULTS AND DISCUSSION

A targeted approach will be preferred if the aim of the study concerns a group of metabolites, for example, amino acids, neurotransmitters, or others. A nontargeted approach will be favored to determine if there is a change in metabolome between various conditions and will then guide a possible targeted approach. Results were analyzed using both targeted and untargeted approaches. The aim of targeted metabolomics is to quantify specific molecules, while untargeted metabolomics aims at screening a maximum of metabolites and identifying the ones that are the most discriminant between several conditions. In LC−MS, due to the physicochemical properties of LC columns, the less polar compounds are mainly retained on an RP−C18 column, while many polar metabolites are eluted near the void volume. The polar compounds are generally retained on an HILIC column, but this chromatography could optionally lead to less reproducible untargeted metabolic profiling and requires longer equilibration time than RP−LC−MS. As no single chromatographic method is ideal to detect all classes of metabolites, the combination of both columns will extend the range of detected molecules in a biological sample.

3.1. Optimization of Extraction

3.1.1. Amniotic Fluid. The AF metabolome has been frequently studied using NMR in clinical and preclinical studies,[11,34] but for the past few years, the use of LC−MS is quickly increasing.[35] Several studies already report the use of

https://doi.org/10.1021/acs.jproteome.1c00145
J. Proteome Res. XXXX, XXX, XXX−XXX

Table 2. Reproducibility Assesment of Metabolites Detected in AF in C18 and HILIC LC−MS Using Untargeted Analyses in ESI+/− Modes (n = 6 Replicates)

AF−untargeted analysis		MeOH		ACN		MeOH/ACN	
		C18	HILIC	C18	HILIC	C18	HILIC
mean total intensity (standard deviation)	ESI+	2.32×10^{10} (5.8×10^{8})	1.26×10^{10} (8.4×10^{8})	2.12×10^{10} (7.9×10^{8})	7.58×10^{9} (1.0×10^{9})	2.33×10^{10} (7.9×10^{8})	7.34×10^{9} (1.3×10^{9})
	ESI−	9.30×10^{9} (2.8×10^{8})	8.83×10^{9} (6.6×10^{8})	8.50×10^{9} (4.7×10^{8})	9.35×10^{9} (8.9×10^{8})	9.06×10^{9} (3.9×10^{8})	1.05×10^{10} (7.4×10^{8})
total features	ESI+	3020	4400	3005	4482	3020	4473
	ESI−	1958	3599	1961	3621	1960	3635
features with CV < 30%	ESI+	1725	1182	1677	2092	1614	1447
	ESI−	1374	1697	1322	1577	1376	1247
percentage of reproducible features	ESI+	57%	27%	56%	47%	53%	32%
	ESI−	70%	47%	67%	44%	70%	34%
mean % CV from reproducible features	ESI+	13.8	18.4	14.9	20.0	14.3	21.5
	ESI−	12.7	18.0	14.7	18.9	13.0	20.4

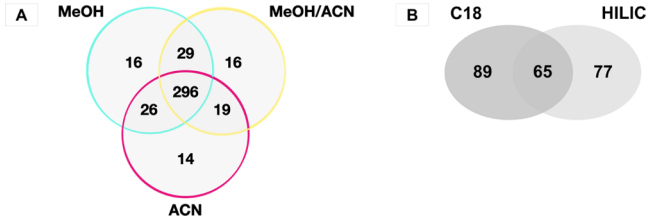

Figure 2. AF analysis using targeted C18 and HILIC LC−MS (ESI +/− modes) (n = 6 replicates): (A) total number of metabolites detected depending on the extraction solvent: MeOH, ACN, or a mixture of both; (B) complementarity of reversed-phase (RP-C18) and HILIC LC−MS from MeOH extraction.

different solvents such as MeOH or ACN to deproteinize and extract metabolites[12,17,36] but without a rationale for their choice. Therefore, we have assessed three extraction methods using MeOH, ACN, or a mixture of both solvents on rat AF samples.

3.1.1.1. LC−MS Analysis. 3.1.1.1.1. Targeted analysis. The solvent extraction efficiency was evaluated through two approaches: *via* the total intensity of the extracted features and *via* the total number of extracted metabolites. In the C18−LC−MS platform, the mean total intensities of all targeted extracted metabolites with MeOH were 8% higher than with ACN and MeOH/ACN extractions; ACN and MeOH/ACN were equivalent. The same trend was observed for reproducible metabolites (with a CV < 30%)[37] (Table 1). The same results were obtained with the untargeted approach (Table 2). These mean intensities were globally 66% higher than with the HILIC−LC−MS platform. Using HILIC−LC−MS, the efficiency of the MeOH extraction was 40% higher than the ACN extraction and was 1% lower than the MeOH/ACN extraction (Table 1).

The total number of metabolites detected in rat AF depended on the solvent for extraction, and their specificity was investigated in targeted analysis (Figure 2). Interestingly, the three solvents were roughly equivalent in regard to the total number of metabolites extracted (Figure 2A), as 81 to 83% of metabolites were commonly detected with each method. Among the 416 metabolites detected regardless of the solvent used for extraction, MeOH was the solvent leading to the highest number of metabolites detected (367) (Figure 2A).

The quality of each extraction was evaluated by the repeatability based on PCA (Supporting Information, Figure S1) and % CV. For the three solvents used, the C18−LC−MS platform detected the highest number of reproducible metabolites (with a CV < 30%) compared to the HILIC−LC−MS platform (Table 1). With the C18−LC−MS platform, the number of reproducible metabolites extracted by MeOH and ACN was equal (167 among 197 annotated metabolites) and slightly lower for MeOH/ACN extraction (157 among 195 annotated) (Table 1), leading to similar total intensities of targeted metabolites with a CV < 30% compared to the total intensity of all metabolites (Table 1). With the HILIC−LC−MC platform, MeOH extracted a higher number of reproducible metabolites (139) compared to 122 reproducible metabolites with ACN extraction and 108 with the mixture of both solvents (Table 1). Among the replicable metabolites extracted with MeOH, 72% were column-specific and 28% were detected using both columns (Figure 2B). These results highlight the importance of combining RP and HILIC

https://doi.org/10.1021/acs.jproteome.1c00145
J. Proteome Res. XXXX, XXX, XXX−XXX

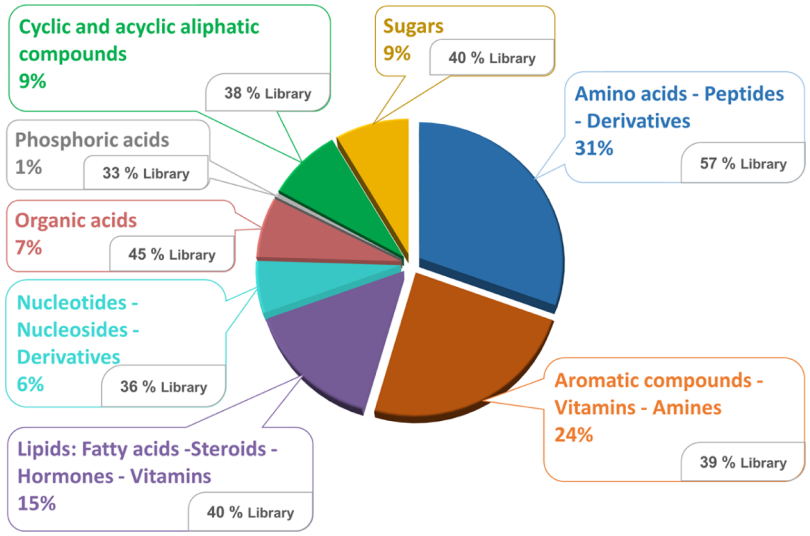

Figure 3. Chemical classes of robust annotated compounds in the AF, extracted with MeOH, and the percentage of the detected compounds relative to the number of metabolites in our library, for each class.

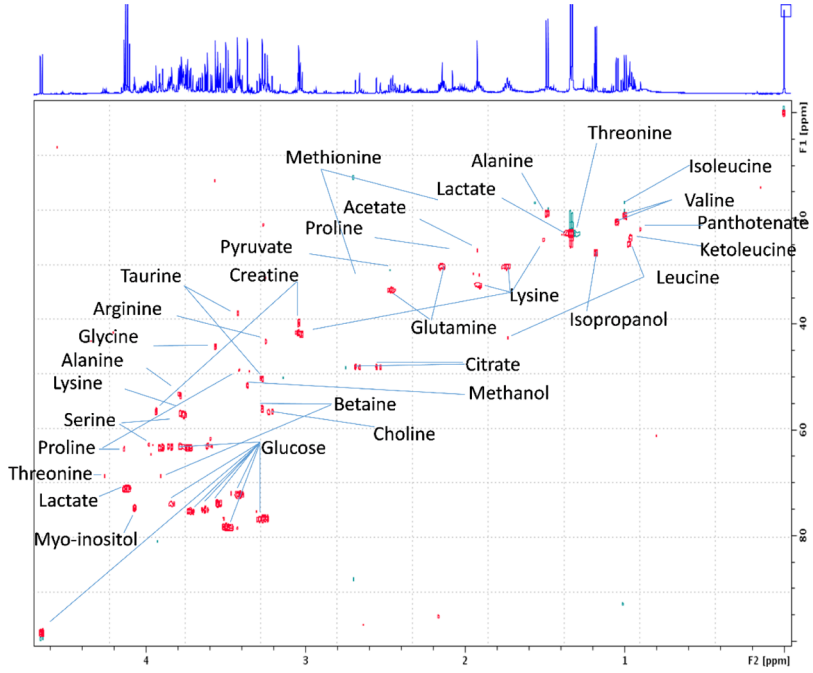

Figure 4. 1D (^{1}H) NMR and 2D heteronuclear (HSQC) spectra of the rat AF sample (150 μL) at 600 MHz and assignment.

chromatography columns for a better metabolome coverage. A list of metabolites detected in AF with MeOH extracting solvent regarding the column and ionization mode is in Supporting Information (Table S1).

Fetal metabolism contributes to the composition of the AF, which changes during gestational stages due to fetal swallowing and lung, urine, and gastric fluid releases. From a MeOH extraction, after data processing (we kept molecules with a CV < 30% in the QC and must respect of the dilution law), 200 unique robust metabolites among 495 molecules of our target library were annotated. About 31% of robust annotated compounds in the AF belong to the amino acid or derivative family, followed by 24% of aromatic compounds and vitamins, and 15% of simple lipids such as fatty acids, steroids, and hormones (Figure 3).

3.1.1.1.2. Untargeted Analysis. The results were similar in the untargeted approach. Using the C18−LC−MS platform, using the untargeted approach, the extraction efficiencies using the total number of features detected were equivalent with each extraction method in ESI+ and ESI− modes (around 3000 and 1960 features, respectively) (Table 2). Considering the reproducible features (with a CV < 30%) of the C18−LC−MS (ESI+) platform, MeOH was a little bit more effective (+48 *vs* +111 features for ACN vs MeOH/ACN extraction methods, respectively) and yielded the highest integrated intensity (+12% *vs* ACN; + 9% *vs* MeOH/ACN). In HILIC−LC−MS (ESI+), around 4450 features were detected with MeOH, providing +910 and +645 reproducibles features compared to ACN and MeOH/ACN extractions, respectively. The same trend was observed in the ESI− mode (Table 2). The numbers of metabolites extracted with MeOH and ACN

https://doi.org/10.1021/acs.jproteome.1c00145
J. Proteome Res. XXXX, XXX, XXX−XXX

Table 3. Reproducibility Assesment of Lipids Detected in the Wet or Lyophilized Placenta in LC−MS (ESI+/− Modes) (Targeted Analyses) (n = 6 Replicates)

placenta lipidomics−targeted analysis (ESI+/−)	CH_2Cl_2		MTBE		BuOH	
	wet	Lyoph	wet	lyoph	wet	lyoph
mean total intensity (standard deviation)	9.37 × 109 (3.2 × 10^9)	5.01 × 109 (8.3 × 10^9)	2.21 × 10^{10} (1.6 × 10^9)	2.45 × 10^{10} (5.9 × 10^9)	9.55 × 109 (2.3 × 10^9)	8.15 × 109 (2.6 × 10^9)
total lipids	247	227	281	277	249	250
percentage of reproducible lipids	61%	72%	68%	51%	41%	52%
mean of % CV from lipids with CV < 30%	20.9	19.8	21.1	21.7	22.1	19.5

were similar to those found in the literature for human AF.[12,36] The three solvents showed a similar reproducibility in targeted C18−LC−MS with a mean % CV of 8%. Using the untargeted approach, the global reproducibility was similar for the three solvents and was higher using the C18−LC−MS analysis compared to the HILIC−LC−MS analysis (CV = 12−14 and 17−21%, respectively).

In conclusion, with regard to extraction efficiency and reproducibility, MeOH and ACN were almost similar. According to specific uses [*e.g.,* only one column, only one approach (targeted/nontargeted), or only one ionization], the choice of the solvent (MeOH *vs* ACN) could be done based on the different tables provided in this study. Taking into account both approaches, both columns, and both ionizations, MeOH was slightly more effective and was therefore chosen for the application experiment described in Section 3.2.

3.1.1.2. NMR. Based on the excellent reproducibility of NMR (*e.g.,* for longitudinal studies), its quantitative accuracy of the analyzed metabolites (*e.g.,* a single internal reference is sufficient for absolute metabolite quantitation over a huge range of concentrations), and its ability to identify structures, NMR 1D (^{1}H) completed by 2D analysis is of a great interest for the metabolome characterization.[38] From native rat AF samples, 41 metabolites were detected in 1D NMR, and five additional metabolites were detected by 2D [these compounds were nonassigned by ^{1}H due to compound overlapping: *O*-phosphoethanolamine, serine, arginine, phosphocholine, and taurine (Supporting Information, Table S2)]. We performed resolution-enhanced 2D NMR using NUS, with no increase in experimental time.[26] Heteronuclear single quantum coherence spectroscopy (HSQC) NMR (Figure 4) provided 34 assignments corresponding to aliphatic compounds, and aromatic metabolites could not be observed at 600 MHz even after 3 h of accumulation. For an analytical comparison, Graça and colleagues described in human AF (but from 1 mL) around 50 molecules detected at 800 MHz.[11] While 18 of these molecules were not observed under our analytical conditions, we annotated 12 other molecules that they were not described in their analysis (see comparison in Table S2, Supporting Information). From the ^{1}D NMR analysis, 91% of the detected molecules were robust, while 14 molecules did not follow a linear dilution curve (from 150, 100, and 50 μL samples). One of the major assets of NMR is to provide simultaneous quantification of routine metabolites. An example of quantification of several rat AF metabolites can be found in Supporting Information (Figure S2). The complementarity of LC−HRMS (C-18 + HILIC, 200 unique metabolites) and NMR (1D + 2D, 46 molecules) showed 19 metabolites analyzed only by NMR (Supporting Information, Figure S3).

3.1.2. Placenta. Due to the high lipid content of the placenta, biphasic extractions such as the Folch method or the Bligh−Dyer method[22,39] and the Matyash method[17] have been performed to collect both the metabolome and lipidome. BuOH/MeOH (BuMe) extraction has been used for plasma lipidomics[40] but has been rarely tried with tissue samples. Few papers described BuMe as an extraction solvent for placenta tissue,[41] and it has not been used for the extraction of both metabolome and lipidome. Therefore, we compared CH_2Cl_2/MeOH, MTBE/MEOH, and BuMe as solvent extractions for both metabolome and lipidome characterizations.

3.1.2.1. Lipidomics. Regarding lipidomics, our results showed that working on the fresh or lyophilized placenta was almost equivalent in regard to total intensity, quantity of

https://doi.org/10.1021/acs.jproteome.1c00145
J. Proteome Res. XXXX, XXX, XXX−XXX

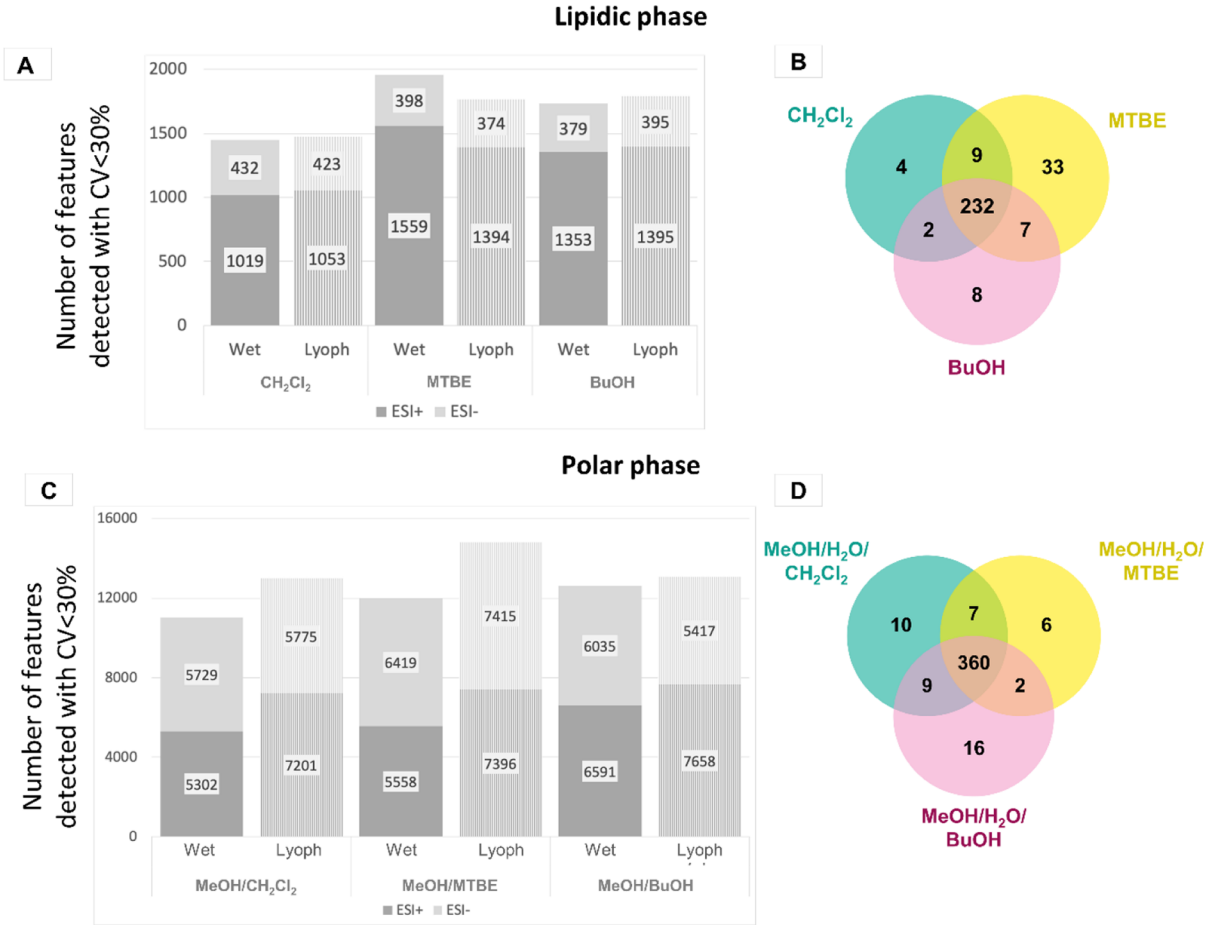

Figure 5. LC−MS analyses (ESI+ and ESI−) of the wet placenta for each lipidome/metabolome extraction solvent: MeOH/CH_2Cl_2, MeOH/MTBE, and MeOH/BuOH (n = 6 replicates). (A) Total number of detected lipidic features; (B) specificity of the extracting solvent on the number of targeted lipids; (C) total number of detected features; and (D) specificity of the extracting solvent on the number of targeted metabolites.

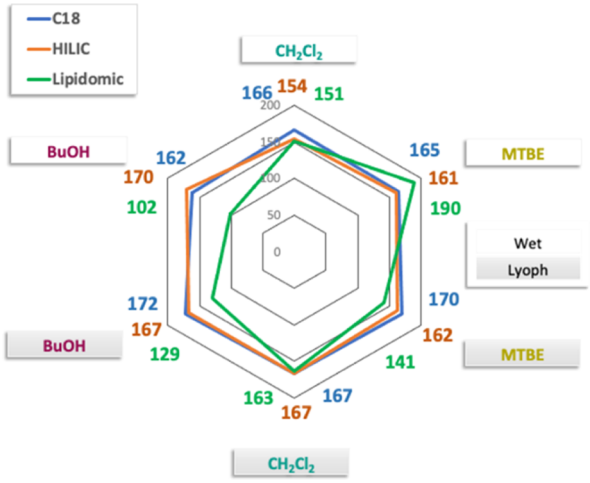

Figure 6. Number of polar metabolites and lipids detected in the placenta using C18 and HILIC LC−MS analyses and lipids in ESI+ and ESI- modes with a CV < 30 % for each extraction solvent: CH_2Cl_2, MTBE, or BuOH (targeted analysis) (n = 6 replicates).

lipids extracted, and reproducibility (% CV), regardless of the solvent used. Indeed, 94 ± 4% of the lipids extracted were observed using both types of samples (Table 3, Figure S4, Supporting Information). In parallel, the multivariate analysis by PCA revealed that the major difference came from the choice of the extracting solvent (MTBE *vs* BuOH and CH_2Cl_2) (PC1 = 0.58), and the lyophilization was much less impactful (Supporting Information, Figure S5).

Using untargeted lipidomics analysis, wet or lyophilized tissue gave the same results when extracted using MeOH or BuOH (Figure 5A, Table S4), but MTBE extraction on wet tissues was slightly more effective with more features detected compared to lyophilized tissue in both targeted and untargeted studies (Figure 6 and Table S4). MTBE extraction also led to higher intensities of lipids than CH_2Cl_2 and BuOH extractions (Table 3, Figures 5 and 6).

Contrary to CH_2Cl_2, MTBE is the upper phase in the biphasic extraction step, which is an important advantage in the experimental process. This could explain the higher robustness of the extraction on the wet placenta [68% of robust lipids (with a CV < 30%) compared to 61% (but 10 time less intense) using CH_2Cl_2 and 41% using BuOH].

3.1.2.2. Polar Metabolomics. Regarding the metabolome, HILIC and C18 LC−MS provided similar results in terms of intensities and the number of detected metabolites for wet or lyophilized placentae as observed by Troisi and collaborators.[42] Furthermore, no notable impact of the lipid solvent extraction was detected as the three protocols led to the same metabolome (Table 4, Figure 5 and Table S3 in Supporting Information). Regarding the detection coverage, from a MeOH/H_2O/MTBE extraction, after drastic data processing (CV < 30% in the QC and the respect of the dilution law),

https://doi.org/10.1021/acs.jproteome.1c00145
J. Proteome Res. XXXX, XXX, XXX−XXX

Table 4. Reproducibility of Detected Metabolites in the Wet or Lyophilized Placenta by C18 and HILIC LC−MS Targeted Analyses (ESI ± Modes), Extracted Using MeOH/H_2O/MTBE (n = 6)

placenta metabolomics−targeted analysis		MeOH/H_2O/MTBE	
		wet	lyoph
mean total intensity (standard deviation)	C18 ESI+/−	1.86×10^{10} (1.6×10^{9})	1.94×10^{10} (7.0×10^{8})
	HILIC ESI+/−	7.53×10^{10} (5.4×10^{9})	7.42×10^{10} (1.3×10^{9})
total metabolites	C18 ESI+/−	189	192
	HILIC ESI+/−	186	184
percentage of reproducible metabolites	C18 ESI+/−	87%	89%
	HILIC ESI+/−	87%	88%
mean % CV from reproducible metabolites	C18 ESI+/−	13.3	8.8
	HILIC ESI+/−	13.2	10.2

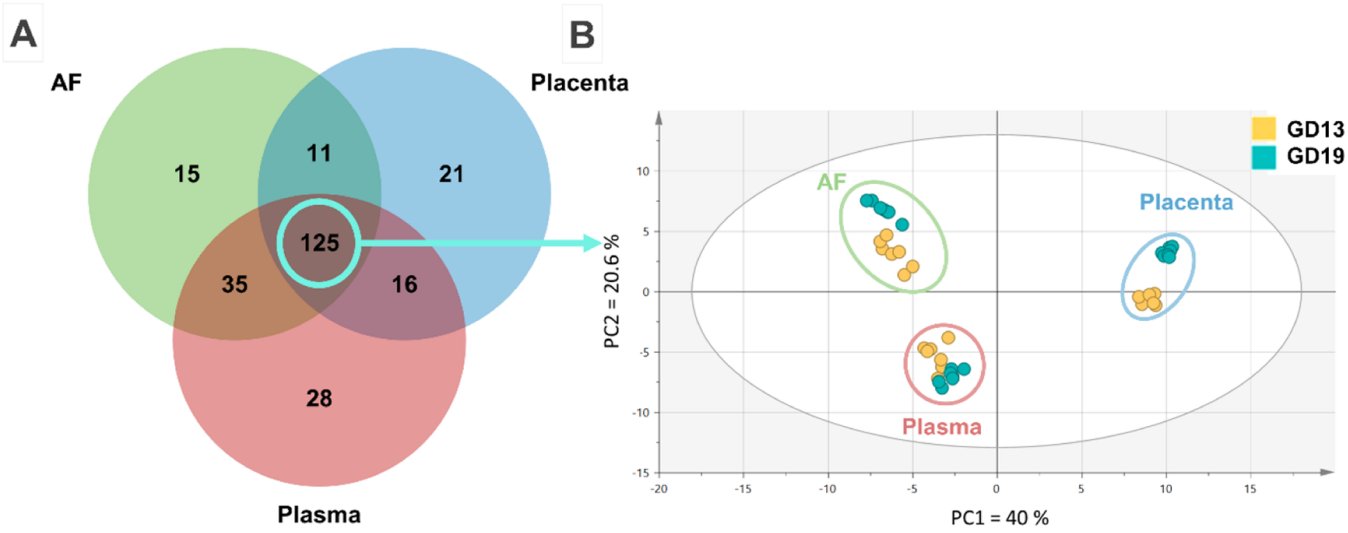

Figure 7. (A) Complementarity of common metabolites detected between AF, placenta, and plasma. (B) Score plot of the PCA of AF, placenta, and plasma at GD13 and GD19 stages, from the 125 common detected metabolites in the three matrices (n = 7 females): R2X(cum) = 0.88 and Q2(cum) = 0.81.

Table 5. Statistical Analysis (Wilcoxon Rank-Sum Test, FDR Corrected p Value) between GD13 and GD19 Stages for Each Matrix with Total Metabolites and Matrix Specific Metabolites (n = 7)

GD13 *vs* GD19 stages	AF	Plasma	placenta	lipidomics placenta
discriminant metabolites p(FDR) < 0.05	88/186 (47%)	72/204 (35%)	136/173 (79%)	276/361 (76%)
stable metabolites p(FDR) > 0.5	49/186 (26%)	38/204 (19%)	24/173 (15%)	28/361 (8%)

about 32% of robust annotated metabolites in the placenta belong to amino acids or derivatives, 21% to aromatic compounds and vitamins, and 14% to small lipids such as fatty acids and hormones. The repartition of the different chemical classes of annotated placenta metabolome was similar to what we observed in the AF (Figure 3).

Considering the efficiency, reproducibility, and the time needed for lyophilization, a biphasic extraction with MTBE on the wet placenta was chosen for the rest of the experiment (see Section 3.2).

3.2. Application: Study of two Gestational Stages

As a proof of concept, the metabolomes of the AF and placenta (n = 7 pregnant rats per group) were compared at two gestational stages, gestational day 13 (GD13) and gestational day 19 (GD19), corresponding to the second month and end of the first trimester of pregnancy in humans, respectively.[18]

To complete the specific maternal compartment metabolic fingerprinting, we also analyzed the plasma profiling to evaluate the complementarity of these different matrices. For each matrix, the number of detected targeted metabolites was similar at both gestational stages, with less than 15% of the metabolites detected at only one stage (data not shown). AF, placenta, and maternal plasma shared 125 targeted metabolites, detected at both stages, but each matrix had some specific metabolites nondetected in other matrices (Figure 7A). Overall, 18% and 14% of the targeted metabolites in the placenta and AF, respectively, were not detected in plasma. Although the metabolic composition of these three matrices was almost similar, the concentrations of the different metabolites were quite different across the studied compartments, as shown in the score plot of the PCA (Figure 7B). PCA demonstrated that each matrix had a specific metabolome, and the first principal component (PC1) showed the metabolic difference between the placenta and the other two matrices accounting for 40% of the total variance (Figure 7B). Even if the specific metabolome of each matrix was dominant, the PCA also showed differences in metabolomes between GD13 and GD19, markedly in the placenta but less observable in the plasma.

https://doi.org/10.1021/acs.jproteome.1c00145
J. Proteome Res. XXXX, XXX, XXX−XXX

Additional statistical analyses were performed, on targeted data, to explore the differences between the two gestational stages in each matrix (Table 5). The main metabolic evolution was observed in the placenta. In the placenta, 79 and 76% of the metabolome and lipidome were significantly different (had different molecular intensities) between GD13 and GD19 ($p < 0.05$). In comparison, 47% of the AF metabolome and only 35% for the maternal plasma metabolome significantly differed between GD13 and GD19. These percentages also reflected the PCA (Figure 7B). The fact that almost half of the targeted metabolites differed between the two stages could be explained by the fact that both maternal and fetus metabolisms occur in these mother−offspring interfaces making it very dynamic.[43] This is consistent with the results observed in women's placental metabolomics by Dunn and collaborators who described important changes in lipid metabolism during the early development of the placenta.[44] This important metabolic evolution of the placenta metabolome is consistent with the wide array of structural and functional modifications of the placenta between these two stages.[45]

The placenta and AF metabolomics also contained metabolites that displayed very little changes between the two gestational stages ($p > 0.5$), revealing metabolic stability. In the AF and maternal plasma, 26 and 19% of the metabolites, respectively, did not change in intensity between the two stages ($p > 0.5$). For the placental metabolome and lipidome, 15 and 8%, respectively, were stable. Interestingly, these stable metabolites were specific to each matrix (79 up to 82% were stable in only one matrix), none of the 125 metabolites was stable over time in the three matrices (Figure S6, Supporting Information).

Even with small samples collected from pregnant rodents, analyzing the metabolomics and lipidomics of the AF and placenta is an efficient tool to study prenatal metabolism evolution in pregnant rats and their fetuses. Even though each matrix had a highly specific metabolic profile, changes in the metabolomics profile over the gestation period were detectable.

4. CONCLUSIONS

As the fetal development depends on maternal−fetal metabolic exchanges, the characterization of metabolic fingerprintings of the placenta and AF can be of a great value. Methods to extract the metabolome from these matrices need to be validated in order to provide the maximum of information and robustness for biological studies. We evaluated the performance of different analytical methods for analysis of rat placenta and AF metabolomes to provide as much information as possible and to help the research community to choose an appropriate method for their studies. The present work showed that MeOH and ACN extraction methods provided similar results and were suitable for studying the AF metabolome. That said, MeOH provided slightly more efficient results for the AF metabolome in both C18− and HILIC−LC−MS platforms, in targeted and untargeted analyses. Despite the nondetection of some ionic metabolites using RP and HILIC chromatographic approaches, and the difficulty of identifying metabolites using an untargeted approach, a good coverage of the metabolome was achieved using a multiplatform LC−MS analysis. NMR allowed us to analyze/quantify in a reproducible way, without any extraction step, 41 metabolites in the AF and was a complementary tool for 10% additional annotated metabolites to those analyzed by the combined C18- and HILIC−LC−MS (ESI+/ESI−). Lyophilization of the placental tissue did not impact the placental metabolome and lipidome, neither did the extraction solvent on the metabolome. However, MTBE provided more complete and reproducible extraction results on the lipidome in both targeted and untargeted analyses. LC−MS analyses of AF and placenta metabolomes allow rat gestational stage discrimination which could be a powerful tool to create a detailed metabolic profiling and identify biomarkers of fetal development and developmental diseases.

■ ASSOCIATED CONTENT

Supporting Information

The Supporting Information is available free of charge at https://pubs.acs.org/doi/10.1021/acs.jproteome.1c00145.

PCA score plot of the targeted AF metabolome using MeOH, ACN, or MeOH/ACN extraction; list of polar metabolites (C18− and HILIC−LC−MS platforms ESI +/− modes); NMR 1D and 2D assignments for rat AF from 150 μL at 600 MHz compared to data from the literature; some AF quantified metabolites by ^{1}H NMR; complementarity between C18- and HILIC−LC−MS and NMR targeted annotation; complementarity between wet or lyophilized tissue for each extraction solvent; reproducibility of metabolites detected in the wet or lyophilized placenta; PCA score plot of placental lipidome with CH_2Cl_2, MTBE, and BuOH extraction solvent on wet or lyophilized tissue; complementarity/specificity between matrices of stable metabolites between GD13 and GD19 stages; and reproducibility of extracted metabolites and lipids in wet or lyophilized placental tissue in untargeted analyses (PDF)

■ AUTHOR INFORMATION

Corresponding Author

Sylvie Mavel − *UMR 1253 iBrain, Université de Tours, Inserm, Tours 37000, France*; orcid.org/0000-0002-1424-2698; Phone: +(33)247366279; Email: mavel@univ-tours.fr

Authors

Alexandra Bourdin-Pintueles − *UMR 1253 iBrain, Université de Tours, Inserm, Tours 37000, France*

Laurent Galineau − *UMR 1253 iBrain, Université de Tours, Inserm, Tours 37000, France*

Lydie Nadal-Desbarats − *UMR 1253 iBrain, Université de Tours, Inserm, Tours 37000, France*

Camille Dupuy − *UMR 1253 iBrain, Université de Tours, Inserm, Tours 37000, France*

Sylvie Bodard − *UMR 1253 iBrain, Université de Tours, Inserm, Tours 37000, France*

Julie Busson − *UMR 1253 iBrain, Université de Tours, Inserm, Tours 37000, France*

Antoine Lefèvre − *UMR 1253 iBrain, Université de Tours, Inserm, Tours 37000, France*

Patrick Emond − *UMR 1253 iBrain, Université de Tours, Inserm, Tours 37000, France; CHRU de Tours, Service de Médecine Nucléaire In Vitro, Tours 37000, France*

Complete contact information is available at: https://pubs.acs.org/10.1021/acs.jproteome.1c00145

https://doi.org/10.1021/acs.jproteome.1c00145
J. Proteome Res. XXXX, XXX, XXX−XXX

Notes

The authors declare no competing financial interest.

■ ACKNOWLEDGMENTS

This work was supported by the "Institut National de la Santé et de la Recherche" INSERM and the University of Tours. We thank the department "Analyse des Systèmes Biologiques" (PST ASB, Université de Tours, France) for their help with sample analyses. A.B.-P. received a grant from the French Ministry for National Education (bourse ministérielle—2019-11).

■ REFERENCES

(1) Zhang, A.; Sun, H.; Wang, P.; Han, Y.; Wang, X. Modern analytical techniques in metabolomics analysis. *Analyst* **2012**, *137*, 293−300.

(2) De Paepe, E.; Van Meulebroek, L.; Rombouts, C.; Huysman, S.; Verplanken, K.; Lapauw, B.; Wauters, J.; Hemeryck, L. Y.; Vanhaecke, L. A validated multi-matrix platform for metabolomic fingerprinting of human urine, feces and plasma using ultra-high performance liquid-chromatography coupled to hybrid orbitrap high-resolution mass spectrometry. *Anal. Chim. Acta* **2018**, *1033*, 108−118.

(3) Shen, L.; Liu, X.; Zhang, H.; Lin, J.; Feng, C.; Iqbal, J. Biomarkers in autism spectrum disorders: Current progress. *Clin. Chim. Acta* **2020**, *502*, 41−54.

(4) Brown, A. G.; Tulina, N. M.; Barila, G. O.; Hester, M. S.; Elovitz, M. A. Exposure to intrauterine inflammation alters metabolomic profiles in the amniotic fluid, fetal and neonatal brain in the mouse. *PLoS One* **2017**, *12*, No. e0186656.

(5) Bardanzellu, F.; Fanos, V. The choice of amniotic fluid in metabolomics for the monitoring of fetus health—update. *Expert Rev. Proteomics* **2019**, *16*, 487−499.

(6) Wang, L.; Han, T.-L.; Luo, X.; Li, S.; Young, T.; Chen, C.; Wen, L.; Xu, P.; Zheng, Y.; Saffery, R.; Baker, P. N.; Tong, C.; Qi, H. Metabolic Biomarkers of Monochorionic Twins Complicated With Selective Intrauterine Growth Restriction in Cord Plasma and Placental Tissue. *Sci. Rep.* **2018**, *8*, 15914.

(7) Mussap, M.; Zaffanello, M.; Fanos, V. Metabolomics: a challenge for detecting and monitoring inborn errors of metabolism. *Ann. Transl. Med.* **2018**, *6*, 338.

(8) Michaels, J.-E. A.; Dasari, S.; Pereira, L.; Reddy, A. P.; Lapidus, J. A.; Lu, X.; Jacob, T.; Thomas, A.; Rodland, M.; Roberts, C. T., Jr.; Gravett, M. G.; Nagalla, S. R. Comprehensive proteomic analysis of the human amniotic fluid proteome: gestational age-dependent changes. *J. Proteome Res.* **2007**, *6*, 1277−1285.

(9) Menon, R.; Jones, J.; Gunst, P. R.; Kacerovsky, M.; Fortunato, S. J.; Saade, G. R.; Basraon, S. Amniotic fluid metabolomic analysis in spontaneous preterm birth. *Reprod. Sci.* **2014**, *21*, 791−803.

(10) Vaughan, O.; Fowden, A. Placental metabolism: substrate requirements and the response to stress. *Reprod. Domest. Anim.* **2016**, *51*, 25−35.

(11) Graça, G.; Duarte, I. F.; Goodfellow, B. J.; Barros, A. S.; Carreira, I. M.; Couceiro, A. B.; Spraul, M.; Gil, A. M. Potential of NMR Spectroscopy for the Study of Human Amniotic Fluid. *Anal. Chem.* **2007**, *79*, 8367−8375.

(12) Virgiliou, C.; Gika, H. G.; Witting, M.; Bletsou, A. A.; Athanasiadis, A.; Zafrakas, M.; Thomaidis, N. S.; Raikos, N.; Makrydimas, G.; Theodoridis, G. A. Amniotic Fluid and Maternal Serum Metabolic Signatures in the Second Trimester Associated with Preterm Delivery. *J. Proteome Res.* **2017**, *16*, 898−910.

(13) Orczyk-Pawilowicz, M.; Jawien, E.; Deja, S.; Hirnle, L.; Zabek, A.; Mlynarz, P. Metabolomics of Human Amniotic Fluid and Maternal Plasma during Normal Pregnancy. *PLoS One* **2016**, *11*, No. e0152740.

(14) Gil, A. M.; Duarte, D. Biofluid Metabolomics in Preterm Birth Research. *Reprod. Sci.* **2018**, *25*, 967−977.

(15) Walejko, J.; Chelliah, A.; Keller-Wood, M.; Gregg, A.; Edison, A. Global Metabolomics of the Placenta Reveals Distinct Metabolic Profiles between Maternal and Fetal Placental Tissues Following Delivery in Non-Labored Women. *Metabolites* **2018**, *8*, 10.

(16) Fattuoni, C.; Mandò, C.; Palmas, F.; Anelli, G. M.; Novielli, C.; Parejo Laudicina, E.; Savasi, V. M.; Barberini, L.; Dessì, A.; Pintus, R.; Fanos, V.; Noto, A.; Cetin, I. Preliminary metabolomics analysis of placenta in maternal obesity. *Placenta* **2018**, *61*, 89−95.

(17) Xie, H.-h.; Xu, J.-y.; Xie, T.; Meng, X.; Lin, L.-l.; He, L.-l.; Wu, H.; Shan, J.-j.; Wang, S.-c. Effects of Pinellia ternata (Thunb.) Berit. on the metabolomic profiles of placenta and amniotic fluid in pregnant rats. *J. Ethnopharmacol.* **2016**, *183*, 38−45.

(18) Rice, D.; Barone, S., Jr. Critical periods of vulnerability for the developing nervous system: evidence from humans and animal models. *Environ. Health Perspect.* **2000**, *108*, 511−533.

(19) Cequier-Sánchez, E.; Rodríguez, C.; Ravelo, A. G.; Zárate, R. Dichloromethane as a solvent for lipid extraction and assessment of lipid classes and fatty acids from samples of different natures. *J. Agric. Food Chem.* **2008**, *56*, 4297−4303.

(20) Diémé, B.; Lefèvre, A.; Nadal-Desbarats, L.; Galineau, L.; Madji Hounoum, B.; Montigny, F.; Blasco, H.; Andres, C. R.; Emond, P.; Mavel, S. Workflow methodology for rat brain metabolome exploration using NMR, LC−MS and GC−MS analytical platforms. *J. Pharm. Biomed. Anal.* **2017**, *142*, 270−278.

(21) Madji Hounoum, B.; Blasco, H.; Nadal-Desbarats, L.; Diémé, B.; Montigny, F.; Andres, C. R.; Emond, P.; Mavel, S. Analytical methodology for metabolomics study of adherent mammalian cells using NMR, GC-MS and LC-HRMS. *Anal. Bioanal. Chem.* **2015**, *407*, 8861−8872.

(22) Dunn, W. B.; Broadhurst, D. I.; Atherton, H. J.; Goodacre, R.; Griffin, J. L. Systems level studies of mammalian metabolomes: the roles of mass spectrometry and nuclear magnetic resonance spectroscopy. *Chem. Soc. Rev.* **2011**, *40*, 387−426.

(23) Broadhurst, D.; Goodacre, R.; Reinke, S. N.; Kuligowski, J.; Wilson, I. D.; Lewis, M. R.; Dunn, W. B. Guidelines and considerations for the use of system suitability and quality control samples in mass spectrometry assays applied in untargeted clinical metabolomic studies. *Metabolomics* **2018**, *14*, 72.

(24) Pezzatti, J.; Boccard, J.; Codesido, S.; Gagnebin, Y.; Joshi, A.; Picard, D.; González-Ruiz, V.; Rudaz, S. Implementation of liquid chromatography-high resolution mass spectrometry methods for untargeted metabolomic analyses of biological samples: A tutorial. *Anal. Chim. Acta* **2020**, *1105*, 28−44.

(25) Gérard, N.; Fahiminiya, S.; Grupen, C. G.; Nadal-Desbarats, L. Reproductive physiology and ovarian folliculogenesis examined via ^{1}H-NMR metabolomics signatures: a comparative study of large and small follicles in three mammalian species (Bos taurus, Sus scrofa domesticus and Equus ferus caballus). *OMICS* **2015**, *19*, 31−40.

(26) Le Guennec, A.; Dumez, J.-N.; Giraudeau, P.; Caldarelli, S. Resolution-enhanced 2D NMR of complex mixtures by non-uniform sampling. *Magn. Reson. Chem.* **2015**, *53*, 913−920.

(27) Guitton, Y.; Tremblay-Franco, M.; Le Corguillé, G.; Martin, J.-F.; Pétéra, M.; Roger-Mele, P.; Delabrière, A.; Goulitquer, S.; Monsoor, M.; Duperier, C.; Canlet, C.; Servien, R.; Tardivel, P.; Caron, C.; Giacomoni, F.; Thévenot, E. A. Create, run, share, publish, and reference your LC-MS, FIA-MS, GC-MS, and NMR data analysis workflows with the Workflow4Metabolomics 3.0 Galaxy online infrastructure for metabolomics. *Int. J. Biochem. Cell Biol.* **2017**, *93*, 89−101.

(28) Nadal-Desbarats, L.; Veau, S.; Blasco, H.; Emond, P.; Royere, D.; Andres, C. R.; Guérif, F. Is NMR metabolic profiling of spent embryo culture media useful to assist in vitro human embryo selection? *MAGMA* **2013**, *26*, 193−202.

(29) Bitar, T.; Mavel, S.; Emond, P.; Nadal-Desbarats, L.; Lefèvre, A.; Mattar, H.; Soufia, M.; Blasco, H.; Vourc'h, P.; Hleihel, W.; Andres, C. R. Identification of metabolic pathway disturbances using multimodal metabolomics in autistic disorders in a Middle Eastern population. *J. Pharm. Biomed. Anal.* **2018**, *152*, 57−65.

https://doi.org/10.1021/acs.jproteome.1c00145
J. Proteome Res. XXXX, XXX, XXX−XXX

(30) Xia, J.; Bjorndahl, T. C.; Tang, P.; Wishart, D. S. MetaboMiner–semi-automated identification of metabolites from 2D NMR spectra of complex biofluids. *BMC Bioinf.* **2008**, *9*, 507.
(31) Chong, J.; Soufan, O.; Li, C.; Caraus, I.; Li, S.; Bourque, G.; Wishart, D. S.; Xia, J. MetaboAnalyst 4.0: towards more transparent and integrative metabolomics analysis. *Nucleic Acids Res.* **2018**, *46*, W486−w494.
(32) Mavel, S.; Nadal-Desbarats, L.; Blasco, H.; Bonnet-Brilhault, F.; Barthélémy, C.; Montigny, F.; Sarda, P.; Laumonnier, F.; Vourc'h, P.; Andres, C. R.; Emond, P. ^{1}H-^{13}C NMR-based urine metabolic profiling in autism spectrum disorders. *Talanta* **2013**, *114*, 95−102.
(33) Bardou, P.; Mariette, J.; Escudié, F.; Djemiel, C.; Klopp, C. jvenn: an interactive Venn diagram viewer. *BMC Bioinf.* **2014**, *15*, 293.
(34) Serriere, S.; Barantin, L.; Seguin, F.; Tranquart, F.; Nadal-Desbarats, L. Impact of prenatal stress on ^{1}H NMR-based metabolic profiling of rat amniotic fluid. *Magma* **2011**, *24*, 267−275.
(35) Shan, J.; Xie, T.; Xu, J.; Zhou, H.; Zhao, X. Metabolomics of the amniotic fluid: Is it a feasible approach to evaluate the safety of Chinese medicine during pregnancy? *J. Appl. Toxicol.* **2019**, *39*, 163−171.
(36) Carraro, S.; Baraldi, E.; Giordano, G.; Pirillo, P.; Stocchero, M.; Houben, M.; Bont, L. Metabolomic Profile of Amniotic Fluid and Wheezing in the First Year of Life-A Healthy Birth Cohort Study. *J. Pediatr.* **2018**, *196*, 264−269.e4.
(37) Want, E. J.; Masson, P.; Michopoulos, F.; Wilson, I. D.; Theodoridis, G.; Plumb, R. S.; Shockcor, J.; Loftus, N.; Holmes, E.; Nicholson, J. K. Global metabolic profiling of animal and human tissues via UPLC-MS. *Nat. Protoc.* **2013**, *8*, 17−32.
(38) Nagana Gowda, G. A.; Raftery, D. Can NMR solve some significant challenges in metabolomics? *J. Magn. Reson.* **2015**, *260*, 144−160.
(39) Chen, S.; Hoene, M.; Li, J.; Li, Y.; Zhao, X.; Häring, H.-U.; Schleicher, E. D.; Weigert, C.; Xu, G.; Lehmann, R. Simultaneous extraction of metabolome and lipidome with methyl tert-butyl ether from a single small tissue sample for ultra-high performance liquid chromatography/mass spectrometry. *J. Chromatogr. A* **2013**, *1298*, 9−16.
(40) Löfgren, L.; Ståhlman, M.; Forsberg, G.-B.; Saarinen, S.; Nilsson, R.; Hansson, G. I. The BUME method: a novel automated chloroform-free 96-well total lipid extraction method for blood plasma. *J. Lipid Res.* **2012**, *53*, 1690−1700.
(41) Pulkkinen, M. O.; Nyman, S.; Hämäläinen, M. M.; Mattinen, J. Proton NMR Spectroscopy of the Phospholipids in Human Uterine Smooth Muscle and Placenta. *Gynecol. Obstet. Invest.* **1998**, *46*, 220−224.
(42) Troisi, J.; Symes, S.; Adair, D.; Colucci, A.; Prisco, S. E.; Aquino, C. I.; Vivone, I.; Guida, M.; Richards, S. Placental tissue metabolome analysis by GC-MS: Oven-drying is a viable sample preparation method. *Prep. Biochem. Biotechnol.* **2018**, *48*, 474−482.
(43) Maltepe, E.; Fisher, S. J. Placenta: the forgotten organ. *Annu. Rev. Cell Dev. Biol.* **2015**, *31*, 523−552.
(44) Dunn, W. B.; Brown, M.; Worton, S. A.; Davies, K.; Jones, R. L.; Kell, D. B.; Heazell, A. E. P. The metabolome of human placental tissue: investigation of first trimester tissue and changes related to preeclampsia in late pregnancy. *Metabolomics* **2012**, *8*, 579−597.
(45) Furukawa, S.; Tsuji, N.; Sugiyama, A. Morphology and physiology of rat placenta for toxicological evaluation. *J. Toxicol. Pathol.* **2019**, *32*, 1−17.

https://doi.org/10.1021/acs.jproteome.1c00145
J. Proteome Res. XXXX, XXX, XXX−XXX